

AMB2022-04 Benchmark Measurements and Challenge Problems

Last updated on 6/17/2022

Modelers are invited to submit simulation results for any challenges they like before the deadline of 23:59 (ET) on July 15, 2022. Tabulated results using the challenge-specific templates are required for most challenge problems and simulation results may be submitted [here](#). An informational webinar for AMB2022-04 will be held on May 5, 2022, from 15:45 – 16:45 Eastern Time. The webinar registration link is [here](#). After the webinar is completed, links to the recorded presentations and to a FAQ page will be added to the AMB2022-04 description page. Additional information may become available later so new versions of this document may be posted. Please check back occasionally.

All evaluations of submitted modeling results will be conducted by the AM-Bench 2022 organizing committee. Award plaques will be awarded at the discretion of the organizing committee. Because some participants may not be able to share proprietary details of the modeling approaches used, we are not requiring such details. However, whenever possible we strongly encourage participants to include with their submissions a .pdf document describing the modeling approaches, physical parameters, and assumptions used for the submitted simulations.

Please note that the challenge problems reflect only a small part of the validation measurement data provided by AM Bench for each set of benchmarks. The Measurement Descriptions section, below, describes the full range of measurements conducted.

AMB2022-04: Mechanical measurement extension to AMB2018-01: laser powder bed fusion (LPBF) 3D builds of nickel-based superalloy IN625 test objects. Detailed descriptions are found below, and simulation results may be submitted [here](#).

Challenges

- Subcontinuum Mesoscale Tensile Test (CHAL-AMB2022-04-MeTT): Predict subcontinuum stress strain behavior, fracture location, and width reduction of as-built IN625 meso-scale specimens. See sections 3.2 and 4.1 for more details.
- Macroscale Tensile Tests at Different Orientations (CHAL-AMB2022-04-MaTO): Predict bulk/continuum stress strain behavior of as-built IN625 tensile specimens at different specimen tensile axis orientations with respect to the build direction. See sections 3.3 and 4.2 for more details.
- Macroscale Compression at Different Temperatures and Orientations (CHAL-AMB2022-04-MaCTO): Predict bulk/continuum stress strain behavior of as built IN625 compression specimens at different specimen compression axis orientations with respect to the build at three temperatures. See sections 3.4 and 4.3 for more details.

1. Overview and Basic Objectives
 2. Build Process and Part Design
 3. Measurement Descriptions
 4. Benchmark Challenge Problems
 5. Data to be Provided
 6. References
-

1. Overview and Basic Objectives

AMB2022-04 is a direct extension to the measurement data provided by AMB2018-01. For AMB2018-01, data were provided for laser powder bed fusion (LPBF) builds of IN625, including powder characterization, detailed information about the build process, in situ measurements during the build, ex situ measurements of the residual stresses, part distortion following partial cutting off the build plate, location-specific microstructure characterization, and microstructure evolution during a post build heat treatment. Here, these data are extended to include mechanical property data for the as-built material.

When the original AMB2018-01 specimens were produced, a full build plate of four bridge specimens was reserved for future use. For AMB2022-04, a set of compression measurements was conducted on test specimens extracted from the front section of a bridge specimen. In situ diffraction measurements of test specimens obtained from a 5 mm leg were carried out during compression testing at the Cornell High Energy Synchrotron Source (CHESS). In addition, two additional build plates of parts designed for mechanical testing were fabricated using the same build machine as AMB2018-01, the same alloy (different powder lot numbers), and the same bulk material scan pattern. These parts were used for macroscopic and mesoscopic mechanical testing, with additional characterization provided by X-ray Computed Tomography (XRCT) and scanning electron microscopy (SEM). All of the mechanical test specimens were measured in the as-built state, with no residual stress anneal.

2. Build Process and Part Design

The build plate reserved from AMB2018-01 and the two new build plates of specimens for mechanical testing were all built on the same EOS M270.[†] The EOS M270 is referred to using the designation CBM, for commercial build machine. To the greatest extent possible, the build parameters and conditions were kept identical between the AMB2018 and AMB2022-04 builds, but new powder lots were required because there was insufficient IN625 powder remaining from AM Bench 2018. In situ thermography and thermocouple measurements were carried out during the AMB2018-01 build but these in situ measurements were not feasible during the fabrication of the two new build plates. However, in situ thermographic data results from other AMB2018-01 builds are described and linked in [Heigel et al. 2020](#).

2.1 Reserved AMB2018-01 Build Plate

Full details of the build plate, part design, IN625 powder, build process, in situ monitoring, and ex situ measurements are available on the AMB2018-01 website [here](#), and in [Heigel et al. 2020](#). This build plate is designated AMB2018-625-CBM-B3.

2.2 Mechanical Test Specimen Build Plates

The two new build plates are designated AMB2022-625-CBM-B1 and AMB2022-625-CBM-B2. Two lots of powder feedstock were used (B1 used lot M051701, and B2 used lot M341901). Both builds used the same laser power, scan speed, and spot size. Scan strategies varied by part.

2.2.1 Feedstock Material: The new AMB2022-04 builds were conducted using IN625 powder from two lots and the chemical compositions are provided in Table 1. The powders were kept sealed in the original shipment containers until use. Virgin powder was used for each build.

Table 1: Powder characterization

| | M051701 | M341901 |
|--|--------------|--------------|
| Chemical Composition | Ni = Balance | Ni = Balance |
| - Values in this table are taken from vendor-supplied data sheets, which utilized ASTM E1479 (inductively-coupled plasma atomic emission spectrometers) for all elements except for using ASTM E1019 (combustion) for C/S and ASTM E1019 (fusion) for O/N. | Cr = 21.54 | Cr = 20.86 |
| - All composition measurements are in mass (weight) percent. | Fe = 0.78 | Fe = 0.62 |
| | Mo = 9.19 | Mo = 9.03 |
| | Nb = 4.13 | Nb = 3.95 |
| | Co = 0.18 | Co = 0.17 |
| | Ti = 0.38 | Ti = 0.35 |
| | Al = 0.32 | Al = 0.31 |
| | Si = 0.14 | Si = 0.07 |
| | Mn = 0.05 | Mn = 0.04 |
| | P < 0.01 | P < 0.010 |
| | Ta = 0.02 | Ta < 0.01 |
| | C = 0.02 | C = 0.01 |
| | S < 0.005 | S < 0.005 |
| | O = 0.01 | O = 0.022 |
| | N = 0.01 | N = 0.008 |

2.2.2 Build parameters: The build parameters are identical to those used for AMB2018-01 and are listed in Table 2.

Table 2: CBM build conditions. *Estimated

| CBM build conditions | |
|--------------------------------------|----------------------------------|
| Infill laser power | 195 W |
| Infill scan speed | 800 mm/s |
| Contour laser power | 100 W |
| Contour scan speed | 900 mm/s |
| Support laser power | 90 W |
| Support scan speed | 450 mm/s |
| Hatch spacing | 100 μm |
| Layer thickness | 20 μm |
| Scan pattern | Part dependent. See Section 2.4. |
| Infill laser diameter* | 100 μm D4s |
| Contour and supports laser diameter* | 80 μm D4s |

| | |
|--------------|----------|
| Inert gas | Nitrogen |
| Oxygen level | ≈ 0.5 % |

2.2.3 Gas flow system: The CBM uses N₂ gas with low velocity flow.

2.2.4 Substrates: Nickel alloy IN625 AM parts are built on a full size (252 mm x 252 mm) 1045 steel alloy build plate.

2.3 Part Layout and Specimen Naming Convention

2.3.1 AMB2018-625-CBM-B3

Figure 1 shows the design of the AMB2018-625-CBM-B3 build plate along with the part naming convention. The part that was used for this set of benchmark measurements is AMB2018-625-CBM-B3-P3. Figure 2 shows the leg numbering convention used. The AMB2022-04 in situ X-ray diffraction measurements during mechanical testing were all conducted using material extracted from the 5 mm leg L4. This leg is designated AMB2018-625-CBM-B3-P3-L4.

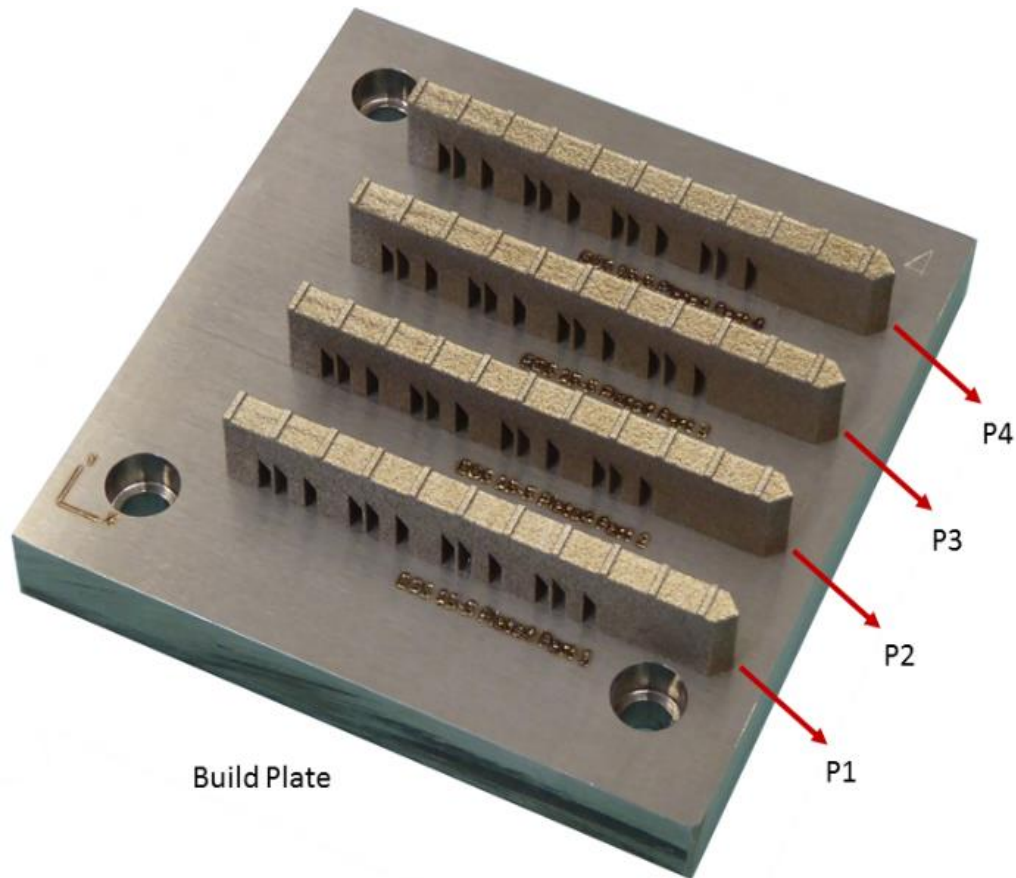


Figure 1: Part numbering for reserved AM Bench 2018 build plate

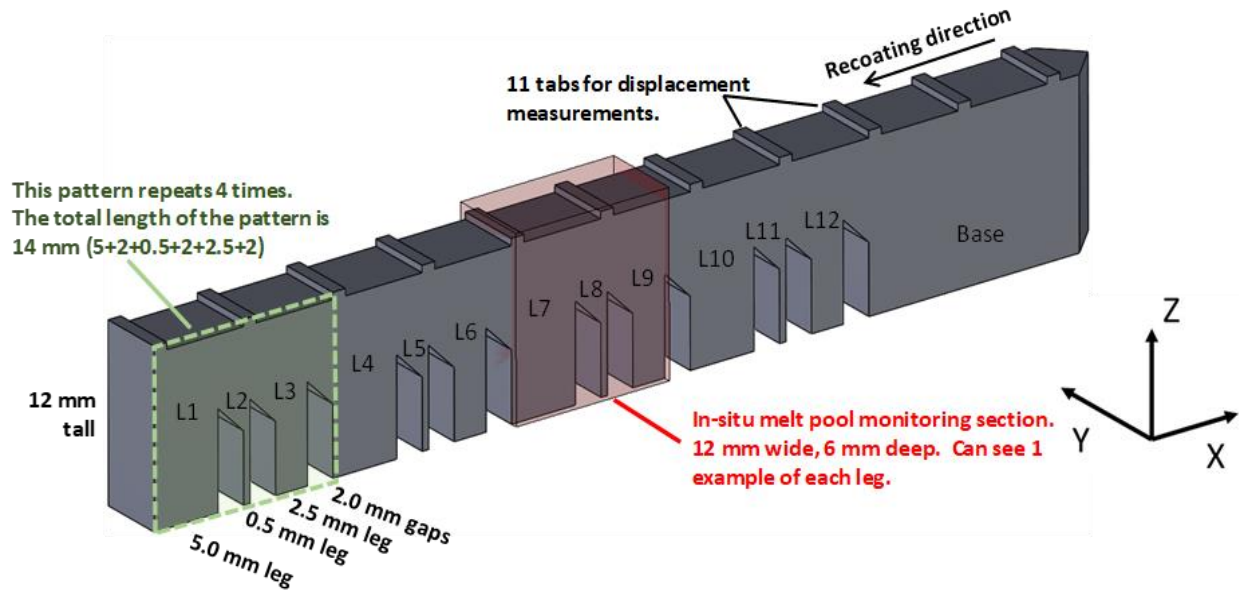


Figure 2: Leg numbering for reserved AM Bench 2018 bridge specimens

Leg L4 was used as source material for 15 “brick” compression specimens, measuring (2.5 x 1.0 x 1.0) mm. Nine specimens were oriented along the build direction (Z axis) and six were oriented along the length of the bridge specimen (X axis). Figure 3 shows a diagram of the sample cutting plan.

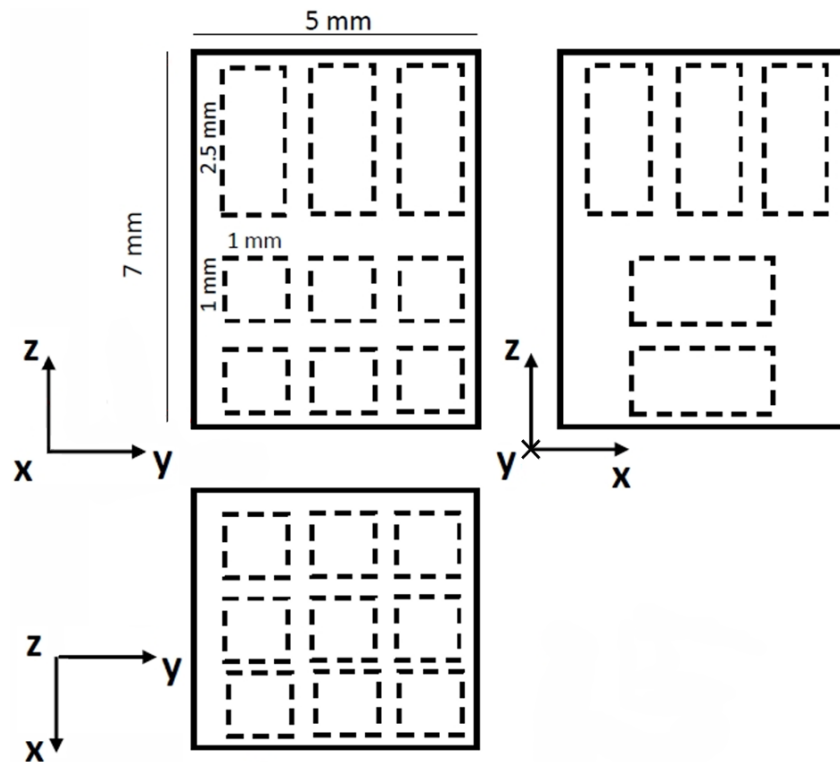


Figure 3: Diagram showing cutting plan for the 15 brick compression specimens

Ten additional cylindrical mechanical test specimens were extracted using wire electrical discharge machining (EDM) from the front section of the part as shown in Fig. 4. Of these, 5 were oriented parallel to the build (Z) axis and 5 were oriented parallel to the Y axis. The sample ends were lapped flat and parallel to within 0.05 mm. The unique specimen IDs are made by appending the sample IDs in Fig. 4 with the part ID. For example, AMB2018-625-CBM-B3-P3-V3 identifies the central vertical specimen and AMB2018-625-CBM-B3-P3-TT1 identifies the leftmost transverse specimen. A mechanical drawing for the cylindrical specimens may be found [here](#).

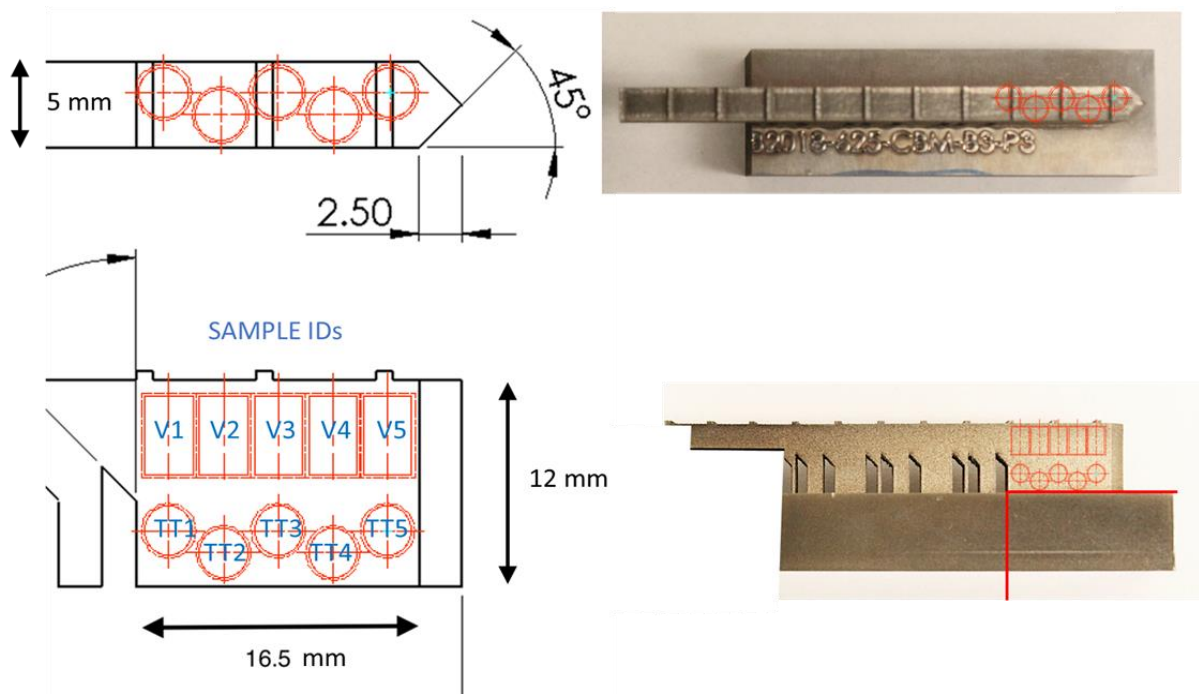


Figure 4: Cylindrical test specimen locations and sample IDs

2.3.2 AMB2022-625-CBM-B1

Figure 5 shows a diagram of the AMB2022-625-CBM-B1 build plate. This plate included 8 macroscale tensile specimens (T1-T8), 3 parts designed to provide material for mesoscale tensile specimens (TH1-3), and several additional parts for general purpose use. The part labels on Fig. 5 are appended to the build plate ID to provide unique identifiers for the individual parts. For example, AMB2022-625-CBM-B1-T7 refers to the macroscale tensile specimen labeled T7 in Fig. 5.

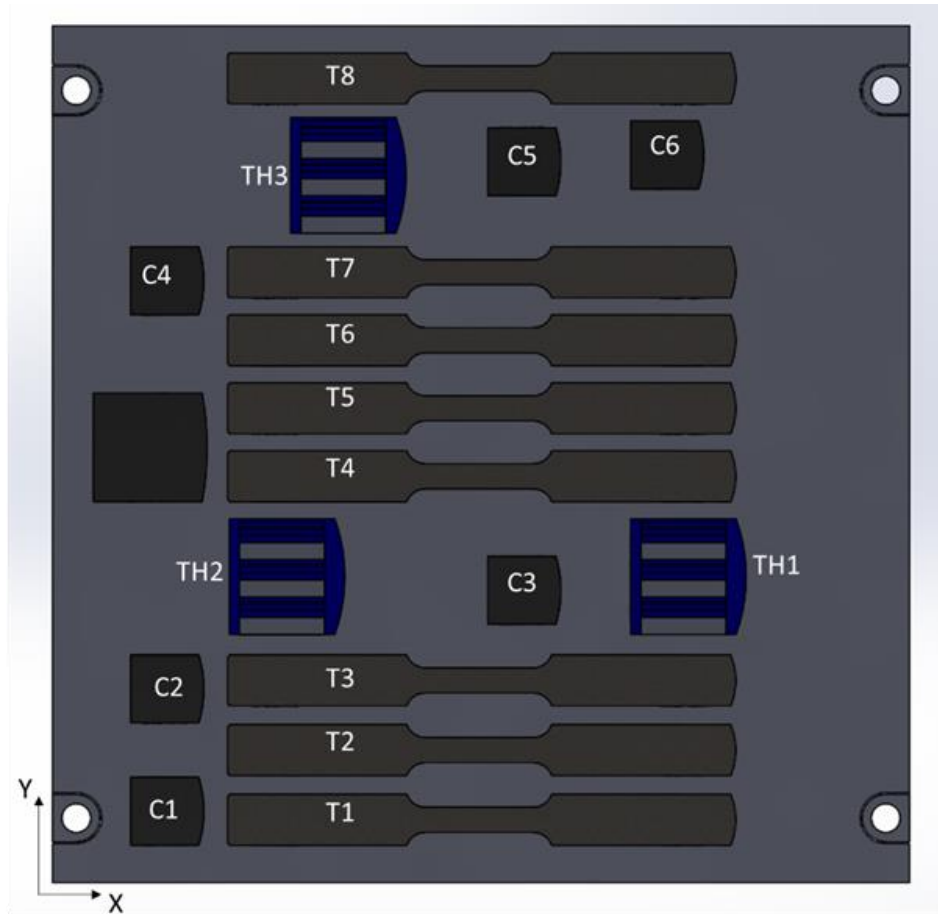


Figure 5: Diagram of AMB2022-625-CBM-B1 build plate

2.3.3 AMB2022-625-CBM-B2

Figure 6 shows a diagram of the AMB2022-625-CBM-B2 build plate. This plate included 3 additional macroscale tensile specimens (T1-T3), 40 parts produced using two different scan strategies that provided material for mesoscale directional tensile specimens (X.01-X.20, XY.01-XY.20), and two additional parts for general purpose use (C1-C2). The part labels on Fig. 6 are appended to the build plate ID to provide unique identifiers for the individual parts. For example, AMB2022-625-CBM-B2-X.12 refers to the part labeled X.12 in Fig. 6.

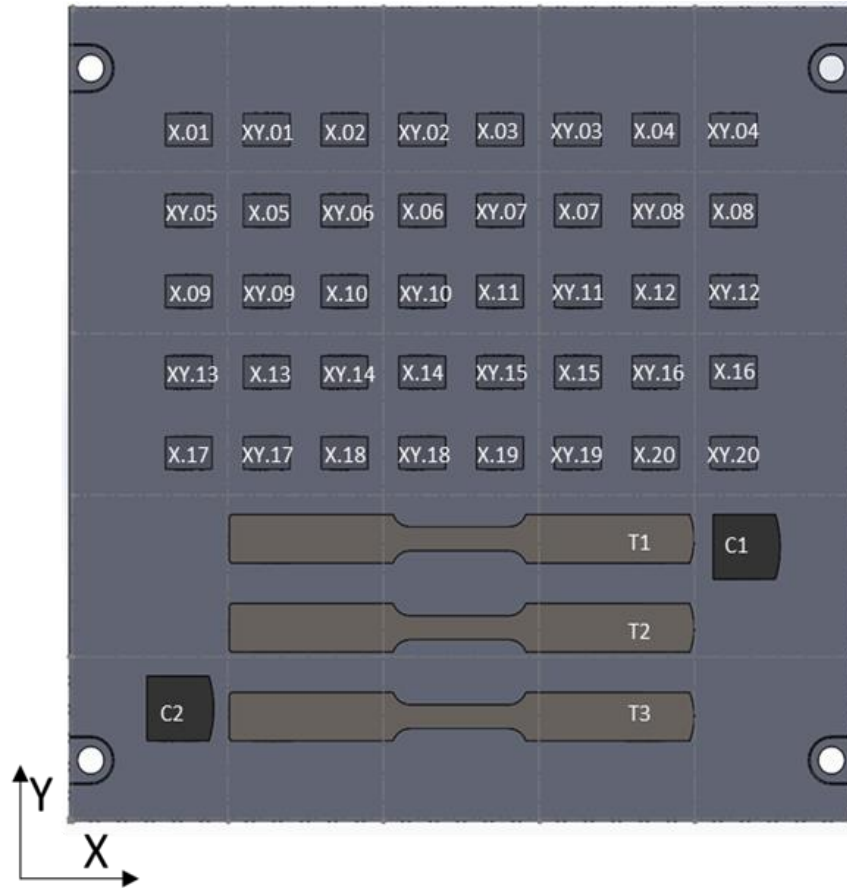


Figure 6: Diagram of AMB2022-625-CBM-B2 build plate

2.4 Scan Strategies

The scan strategy used for the reserved AMB2018-01-625-CBM-B3 build plate was thoroughly documented previously, with details available on the AMB2018-01 website [here](#), and in [Heigel et al. 2020](#).

For the new AMB2022-625-CBM-B1 build plate, parts were built using the same pre-contour and alternating XY scan strategy used for the AMB2018-01 builds. However, for the macro-tensile bars the odd layers alternate between an A and B pattern as shown in Figure 7 where the scan pattern rotates 180° between odd layers. Additionally, the three wall sizes in the thin wall design parts labeled TH1, TH2, and TH3 in Fig. 5 used an X-scan only. The supporting material was built using a default scan pattern with a 67° rotation between layers, 4 mm stripe width, and default skin post-contour (120 W, 900 mm/s). A 100 mm stripe width was used for all the other parts. The parts were located such that the gage sections and thin walls do not contain stripe boundaries.

For the new AMB2022-625-CBM-B2 build plate, parts were built using the same pre-contour and alternating XY scan strategy used for the AMB2018-01 builds as well as an X-scan only strategy. The scan strategy for each block is indicated with an XY or X before the sample number. These 40 blocks do not contain stripe boundaries. The build terminated at a final layer height of 19.06 mm rather than the designed 20 mm due to not enough powder in the dispenser bin.

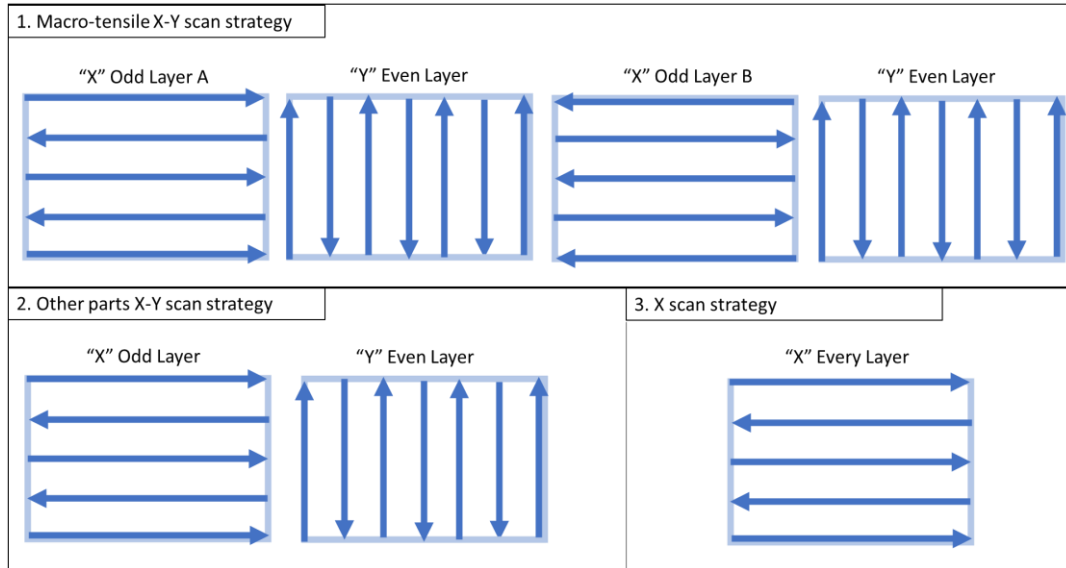


Figure 7: Relative scan strategy orientations for example macro-tensile specimens and AMB2018-01 3D builds

3. Measurement Descriptions

3.1 Macroscale Tensile Tests at Different Crosshead Speeds of AMB2022-CBM-B1 Specimens T1-T8

Five ASTM E8 tensile specimens with a gauge width of 6 mm and a gauge thickness of 4 mm were tested in the as-built condition at room temperature. The specimens were additively manufactured oversized with a build height of ≈ 8.5 mm as shown in Fig. 5. The 4 mm thick specimens were EDM machined 1 mm below the top surface of the build. The gauge section of each sample was then machined using computer numerical control (CNC) milling to the dimensions reported in ASTM E8 for a 6 mm gauge width. Specimens T3, T4, and T6 were tested at a nominal strain rate of 10^{-3} s^{-1} and specimens T5 and T7 were tested at a nominal strain rate of 10^{-2} s^{-1} on a servo-hydraulic material testing machine using a constant crosshead displacement rate of 0.03175 mm/s and 0.3175 mm/s, respectively. Stereo digital image correlation (3D-DIC) was used to report a virtual extensometer strain for a 25.4 mm gauge length up to fracture. The 3D-DIC was measured on the surface that was closest to the top of the build.

3.2 Subcontinuum Mesoscale Tensile Test of AMB2022-CBM-B1 Specimen TH1

This section is only a brief summary of the measurements for this challenge. Please see the NIST Public Data Repository for this challenge (<https://doi.org/10.18434/mds2-2587>) for more detailed information and all data†. One mesoscale tensile specimen (gauge dimensions approximately 0.2 mm x 0.2 mm x 1 mm) was extracted from specimen AMB2022-625-CBM-B1-TH1 (Figure 5) and tested at room temperature using a quasistatic strain rate of 0.001/s to failure. Microstructure was measured using XRCT and SEM techniques on the specimen gauge section or adjacent material. Large-area electron backscatter diffraction was used to measure crystallographic texture and grain size/morphology of the entire gauge section and two orthogonal planes. Backscatter electron imaging was used to characterize the subgrain structure and assess recast layer thickness from electric discharge machining. High energy x-ray diffraction was used to estimate dislocation density. XRCT was used to analyze the pore population as well as uncertainty in cross-sectional area for stress calculations. Literature sources were used to estimate phase fraction, residual stress, and the single crystal C-tensor.

3.3 Macroscale Tensile Tests at Different Orientations of AMB2022-CBM-B2 Blocks X.01-X.20 and XY.01-XY.20

This section is only a brief summary of the measurements for this challenge. Please see the NIST Public Data Repository for this challenge (<https://doi.org/10.18434/mds2-2588>) for more detailed information and all data. Blocks were built with two different scan strategies (Figure 7): XY (blocks XY.01-XY.20 on Figure 6) and X-only (blocks X.01-X.20 on Figure 6). 96 tensile specimens were extracted from blocks at different orientations of the tensile axis with respect to the build direction to yield the following conditions: XY scan strategy (0°, 30°, 45°, 60°, and 90° orientation w.r.t. build direction) and X-only scan strategy (0°, 60°, 90° orientation w.r.t. build direction). Tensile testing was performed at room temperature using a quasistatic strain rate of 0.001/s to failure. Microstructure was measured using XRCT and SEM techniques on representative specimens of each scan strategy. Large-area electron backscatter diffraction was used to measure crystallographic texture and grain size/morphology for three orthogonal planes. Backscatter electron imaging was used to characterize the subgrain structure and assess recast layer thickness from electric discharge machining. High energy x-ray diffraction was used to estimate dislocation density. XRCT was used to analyze the pore population. Literature sources were used to estimate phase fraction, residual stress, and the single crystal C-tensor.

3.4 Compression measurements of AMB2018-625-CBM-B3 cylindrical specimens

The ten cylindrical compression specimens shown in Fig. 4 were tested at room temperature, 250 °C and 500 °C using a quasistatic strain rate of 0.001/s. Testing was performed on a computer controlled electro-mechanical test machine¹ with a high temperature environmental chamber installed. The specimens were loaded in a subpress between tungsten carbide platens. Dry film moly disulfide was used to lubricate the ends of the specimens for room temperature tests, whereas a boron nitride lubricant was used for the 250 °C and 500 °C specimens. Load was measured using the system load cell; an Epsilon model 7642† high temperature extensometer was used to measure relative displacement of the subpress platens. Elevated temperature tests were performed using a constant crosshead displacement rate. Specimens V3 and TT3 were tested in strain control which resulted in a faster displacement rate prior to yield. Temperature measurements were made with type K thermocouples and recorded with an external data acquisition system. One thermocouple was intrinsically welded to the subpress base. A metallic crimp of similar size to the specimen was attached to the tip of the second TC at the sub press. The TC at the subpress was then attached by weld to the top half of the subpress, using a steel wire. The largest masses within the test setup took about 2 h to get to temperature. A soak of 15 min to 20 min was performed before the start of each test. Data collection rate was set to 10 Hz with temperature data being collected at a rate of 1 Hz. All test specimens were successfully tested to about 30 % strain and manually unloaded at the same rate.

3.5 Deformation with in-situ diffraction

A series of *in situ* diffraction measurements were performed during room and elevated temperature compression tests of 'brick' IN625 specimens at the Cornell High Energy Synchrotron Source (CHESS). These data sets are being included in the AM Bench 2022 repositories but are not being used for the

¹ Instron Model No:1127 calibrated 06/25/20, tolerance ± 1% ; Epsilon Model 7642 calibration checked before use using Epsilon Displacement Calibrator A5414 calibrated 09/16/21, tolerance ± 1%.

challenge problems. Specimens were extracted from Leg L4 of the AM bridge specimen (see above for description). A matrix of temperatures, RT, 250 °C, and 500 °C, and engineering strain rates, 10^{-4} 1/s, 10^{-3} 1/s, and 10^{-2} 1/s (build direction specimens only), were utilized for the compression tests to provide a wide range of data for model validation. The thermomechanical tests were performed at the FAST beamline (ID-3A) at CHESS using the RAMS2 load frame and furnace developed by the Air Force Research Laboratory in conjunction with CHESS. Prior to thermomechanical testing, a dummy IN625 specimen extracted from material produced using the same build parameters as the AM Bench bridge specimen was used to calibrate the temperature of the RAMS2 furnace. Diffraction measurements were performed as the furnace was heated, and lattice expansion (i.e., coefficient of the thermal expansion) determined from these diffraction measurements was used to correlate the specimen temperature with reference furnace temperature. After furnace calibration, the thermomechanical test matrix was executed. For each specimen, pole figure measurements were collected prior to loading to characterize the local preferred crystallographic orientation of each specimen. Each specimen was then loaded to approximately 5 % engineering strain after accounting for machine compliance. During specimen loading, diffraction images were collected at a rate of 5 Hz for all tests. This imaging rate provided from 50 to 5000 diffraction images per test depending on the engineering strain rate. Diffraction images were collected on a DEXELA† 2923 area detector sitting 675 mm behind the specimen.

Macroscopic displacement and load applied were also measured simultaneously to diffraction measurements. All macroscopic loading data has been processed into the form of engineering stress-strain curves. From the diffraction images, lattice strains (directional elastic strains with contributions from crystallographic fibers of grain orientation) as a function of applied macroscopic strain were extracted along the loading and transverse-to-loading directions. In particular, lattice strains from representative (i.e., sufficient amounts of intensity along a sample direction of interest) sets of grains with the {111}, {200}, {220}, and {331} lattice planes along the loading and transverse-to-loading direction were collected.

4. Benchmark Challenge Problems

4.1 Subcontinuum Mesoscale Tensile Test (CHAL-AMB2022-04-MeTT)

This section is only a brief summary of this challenge. Please see the NIST Public Data Repository for this challenge (<https://doi.org/10.18434/mds2-2587>) for more detailed information and all data. All processing details, specimen preparation details, tensile test method details, and microstructure measurements are provided. Predictions are requested for the subcontinuum stress strain behavior, fracture location, and width reduction of one as-built IN625 meso-scale specimen.

4.2 Macroscale Tensile Tests at Different Orientations (CHAL-AMB2022-04-MaTTO)

This section is only a brief summary of this challenge. Please see the NIST Public Data Repository for this challenge (<https://doi.org/10.18434/mds2-2588>) for more detailed information and all data. All processing details, specimen preparation details, tensile test method details, and microstructure measurements are provided for both XY and X-only scan strategies. Additionally, true stress-true strain curves for all XY-scan strategy, 0° orientation specimens are provided. Predictions are requested for the bulk/continuum stress-strain behavior of as-built IN625 tensile specimens at different orientations (XY-

scan strategy 30°, 45°, 60°, 90° orientation w.r.t. build direction) and scan strategy (X-only scan strategy 0°, 60°, and 90° orientation w.r.t. build direction).

4.3 Macroscale Compression at Different Temperatures and Orientations (CHAL-AMB2022-04-MaCTO)

This challenge will be to predict the macroscopic stress-strain response of compression samples across a range of temperatures taken from the base leg of the IN625 AMB2018-01 build (<https://www.nist.gov/ambench/amb2018-01-description>) in both the build direction (Z-axis) and a transverse-build direction (Y-axis). The specific temperatures of interest are 298 K, 523 K, and 773 K. The template for submitting the simulation results may be found [here](#).

Data provided will be compared against experimental tests described in Section 3.4 of this document. The exact comparison mapping is provided in Table 3.

Table 3: Sample ID to experimental sample ID mapping

| Sample ID | BD-298K | BD-523K | BD-773K | TD-298K | TD-523K | TD-773K |
|------------------------|---------|---------|---------|---------|---------|---------|
| Experimental Sample ID | V3 | V1 | V2 | TT3 | TT1 | TT2 |

Calibration data will be provided to users which corresponds to the build direction compression tests done at 298 K and 773 K. Please see the NIST Public Data Repository for this challenge (<https://doi.org/10.18434/mds2-2681>) for the calibration data. Users might also find the [previously released and published information](#) related to the AMB2018-01 build useful in completing this challenge.

5. Description and Links to Associated Data

5.1 Subcontinuum Mesoscale Tensile Test (CHAL-AMB2022-04-MeTT)

Please see the NIST Public Data Repository for this challenge (<https://doi.org/10.18434/mds2-2587>) for detailed information and all data.

5.2 Macroscale Tensile Tests at Different Orientations (CHAL-AMB2022-04-MaTTO)

Please see the NIST Public Data Repository for this challenge (<https://doi.org/10.18434/mds2-2588>) for detailed information and all data.

5.3 Macroscale Compression at Different Temperatures and Orientations (CHAL-AMB2022-04-MaCTO)

Please see the NIST Public Data Repository for this challenge (*to be added when available*) for detailed information and all data.

6. References

Citations are provided throughout this document as hyperlinked URLs to the associated digital object identifier (DOI). Clicking this hyperlinked text should open the associated publication or cited source.

†Disclaimers

Certain commercial entities, equipment, or materials may be identified in this document to describe an experimental procedure or concept adequately. Such identification is not intended to imply recommendation or endorsement by the National Institute of Standards and Technology, nor is it intended to imply that the entities, materials, or equipment are necessarily the best available for the purpose.

The National Institute of Standards and Technology (NIST) uses its best efforts to deliver high-quality copies of the AM Bench database and to verify that the data contained therein have been selected on the basis of sound scientific judgment. However, NIST makes no warranties to that effect, and NIST shall not be liable for any damage that may result from errors or omissions in the AM Bench databases.